JOURNAL OF SPACECRAFT AND ROCKETS
Vol. 48, No. 1, January–February 2011

Target Simulator for Serviceability Check of Infrared-Guided Missiles

Anil Kumar Maini*
Laser Science and Technology Centre, Delhi 110 054, India
Anandi Lal Verma
Amity University, Noida, Uttar Pradesh 201 303 India
and
Varsha Agrawal
Laser Science and Technology Centre, Delhi 110054, India

DOI: 10.2514/1.49648

Infrared-guided missiles, along with laser-guided munitions, are the most widely used guided weapons on land, sea, and airborne platforms, due to their precision-strike capability. In view of tactical importance and high cost, these weapons need to be tested at regular intervals. There is always need for portable test systems to perform preflight serviceability checks without removing the weapon from the launch platform. Surface-to-air and air-to-air infrared-guided missiles make use of infrared emission in the 3–5 μm band in the case of single-color missiles and in both 3–5 and 8–12 μm bands in the case of two-color missiles to home in on the target. This paper presents details of two design concepts for building a portable infrared target simulator. The designs were configured around two-dimensional arrays of graybody emitters and a hybrid combination of infrared light-emitting diodes and graybody emitters. The experimental hardware, built to validate the design concepts, was extensively evaluated for its performance parameters using suitable instrumentation. The hardware was used to perform serviceability check of a test missile. Test and evaluation results are presented in the paper.

Nomenclature

c	=	speed of light (3×10^8 m/s)
$f(\lambda)$	=	fractional emissive power (dimensionless)
k	=	Boltzmann constant (1.38×10^{-23} JK^{-1})
n	=	refractive index of the medium (dimensionless)
$P(T)$	=	total power emitted by the graybody element, W
T	=	absolute temperature of the element, K
ε	=	emissivity of the radiating element (dimensionless)
λ	=	wavelength, nm
σ	=	Stefan–Boltzmann constant (5.67×10^{-8} Wm^2 K^{-4})

Introduction

BECAUSE of their precision-strike capability, infrared-guided missiles are among the most commonly exploited class of guided weapons against aerial targets [1]. Infrared-guided missiles make use of the target emission spectra in the 3–5 μm band or in the 3–5 and the 8–12 μm bands [2]. In view of their tactical importance and also for economic reasons, it becomes pertinent that they are tested at regular intervals, and their effectiveness is nearly guaranteed by having the capability to perform prelaunch functionality checks in the strap-on condition. These functional checks, also referred to as serviceability checks, perform go/no-go testing of the weapon by focusing on the most important functional parameters of the guided weapon. When performed just before the mission takeoff, these tests give additional confidence to the mission crew on the strength of their weaponry. When it comes to testing infrared-guided missiles, be it preflight functionality check or comprehensive characterization, the parameters that stand out include spectral matching of received infrared signatures with those of the target known to the seeker, response of the seeker head to target signatures in the presence of static infrared background noise, and immunity to deception by flares and field of view. Out of these four parameters, spectral matching can be singled out as the one to be used for prefunctionality checks, and all four may be evaluated in the case of comprehensive characterization.

The design of the infrared target simulator proposed here for the preflight serviceability check must address both infrared-guided missiles employing single-color seekers and those employing two-color seekers. This implies that the device should be capable of generating target signatures in the 3–5 μm band (for testing single-color infrared-guided missiles) and in the 3–5 and 8–12 μm bands simultaneously (for testing two-color infrared-guided missiles), preferably in the presence of infrared background emission, with desired power density levels. In essence, the device used to perform the serviceability test checks the lock-on sensitivity of the weapon and its ability to perform satisfactorily in the presence of static background noise.

Infrared target simulators designed to characterize infrared-guided missiles are available from international manufacturers such as CI Systems (Israel) and Geotest-Marvin Test Systems, Inc., (United States). Test systems offered by these companies range from simple infrared sources for checking lock-on sensitivity of infrared seekers, intended to be used for performing preflight functionality checks on single- and two-color infrared-guided missiles, to more elaborate systems that generate an infrared scene, which includes a static background, target, and flare signatures. The latter class of test systems is meant for comprehensive characterization of the guided weapon. Some of the better-known commercial systems available for testing infrared-guided missiles include an infrared target simulator and infrared target generator [3], both from CI Systems, and an MTS-16 target simulator from Geotest-Marvin Test Systems, Inc. Most of these systems suffer from one or more of the limitations when it comes to their applicability to perform serviceability check in strap-on condition on both single-color and two-color infrared-guided missiles.

The design concepts presented in this paper can be used to build infrared target simulators that overcome the limitations of similar devices available in the current state of the art. These designs lead to portable test devices to facilitate employment for preflight serviceability checks of single-color and two-color infrared-guided

Received 26 February 2010; revision received 18 September 2010; accepted for publication 21 September 2010.

*Director; akmaini@lastec.drdo.in.

missiles in the presence of static infrared background. The proposed designs are configured around a two-dimensional array of infrared-emitting elements. Different elements are used to generate infrared signatures of the target in the 3–5 and 8–12 μm bands and also infrared background emission in the 3–12 μm band. In the first design, solid-state graybody-emitting elements are used to generate both infrared signatures of the target and those of the background. In the second design, the two-dimensional array is a heterogeneous mix of infrared light-emitting diodes (LEDs) and graybody emitters. Infrared signatures of the target are generated using infrared LEDs with peak emission wavelengths spread over 3–5 μm band, and infrared background emission is generated using a graybody emitter. The LED-based design as of now is applicable to testing of single-color infrared-guided missiles only due to nonavailability of suitable LEDs in the 8–12 μm band.

Design Concepts

Emission in the 3–5 and 8–12 μm bands is characteristic of electromagnetic emission from jet exhaust and mainframe of the aircraft. Spectral content of infrared emission as received by the infrared seeker head is the superposition of spectral emission of the aircraft on the transmission window of the atmosphere [4]. Figure 1 shows the infrared signatures of a typical target aircraft as seen by the seeker head of an infrared-guided missile. Nonimaging types of infrared-guided missiles make use of these infrared signatures to home in on the intended target aircraft. In a real scenario, these infrared signatures are seen against a background with a broadband infrared spectrum. The advances in infrared detectors have increased the detection capabilities of missiles against background noise, resulting in enhancement of their operational ranges [5].

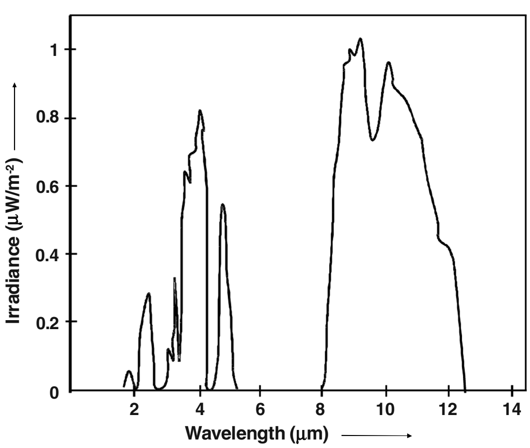

Fig. 1 Infrared signatures of typical target aircraft as seen by seeker head of an infrared-guided missile.

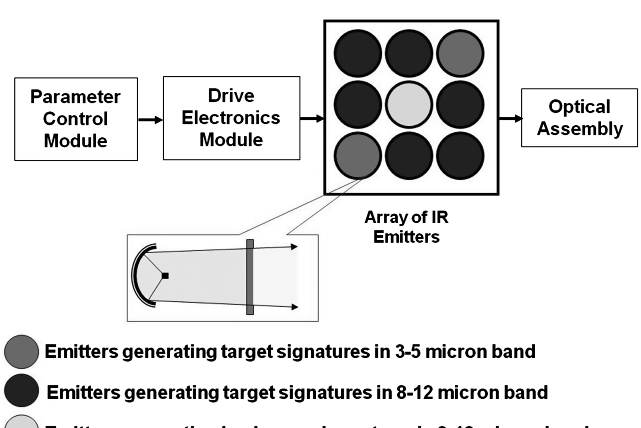

Fig. 2 Block schematic arrangement of design concept using array of graybody radiators.

Design Using Array of Graybody Emitters

A simple infrared target simulator for performing the preflight serviceability check on nonimaging type of single-color and two-color infrared-guided missiles is designed as follows. We configure a two-dimensional array of graybody emitters with different elements driven to generate infrared radiation containing specified amplitudes of target signatures in the 3–5 and 8–12 μm bands and static background infrared noise in the 3–12 μm band. The design offers the flexibility to generate different ratios of the signatures in the 3–5 and 8–12 μm bands to simulate different operational scenarios. Figure 2 shows the block schematic arrangement depicting the concept of the proposed electro-optic device. Major building blocks include array of emitters, parameter control module and drive electronics module to operate the array of emitters, and optical assembly to generate the desired spectral shape. The emitters used here are solid-state emitters whose temperature can be controlled by the dc voltage applied to them. As we know, the infrared radiation emitted by any object and its peak wavelength is related to its temperature by Planck's law and Wein's displacement law, respectively [6,7].

Power emitted by individual graybody emitters between two wavelengths λ_1 and λ_2 is computed from Eqs. (2–4). Fractional emissive power $f(\lambda)$ is defined as the ratio of the emissive power emitted between 0 and λ to the total power $P(T)$ emitted by the element. $P(T)$ is given by Eq. (1):

$$P(T) = \varepsilon\sigma T^4 = n^2\sigma T^4 \tag{1}$$

Power emitted between wavelengths λ_1 and λ_2 is computed from Eqs. (2–4):

$$\int_{\lambda_1}^{\lambda_2} P(\lambda, T)\,\mathrm{d}\lambda = [f(\lambda_2) - f(\lambda_1)]P(T) \tag{2}$$

$$f(\lambda_1) = \int_0^{n\lambda_1 T} \frac{2\pi hc^2\,\mathrm{d}(n\lambda T)}{(n\lambda T)^5\sigma(e^{\frac{hc}{nk\lambda T}} - 1)} \tag{3}$$

$$f(\lambda_2) = \int_0^{n\lambda_2 T} \frac{2\pi hc^2\,\mathrm{d}(n\lambda T)}{(n\lambda T)^5\sigma(e^{\frac{hc}{nk\lambda T}} - 1)} \tag{4}$$

The change of variables to integrate with respect to $n\lambda T$ is done for ease of calculation.

The infrared radiation emitted by these emitters is controlled by the dc voltage fed to them. The proposed design concept was evaluated by using a 3×3 array with two of the nine emitters used for generating the spectrum in the 3–5 μm band, six emitters used for generating the spectrum in the 8–12 μm band, and a single emitter in the center of the array to generate the infrared background emission. This design is a significant upgrade of an earlier design suggested by Maini et al. [8]. Though the hardware built to validate the proposed design concept of the infrared target simulator is configured around a 3×3 array of graybody emitters, the concept is equally valid for two-dimensional array of infrared emitters of any size using other types of infrared emitters, as long as it meets the requirement of producing the required power density in the given spectral band along with the desired spectral shape.

In the two-dimensional array of infrared emitters, emitters used for generating spectra in the 3–5 and 8–12 μm bands are used along with parabolic reflectors to reduce the divergence to generate the desired spot size. The divergence of these emitters is $\pm 50°$ without the reflector and $\pm 15°$ with the parabolic reflector. The parabolic reflector transforms the spherical wave generated by a point source placed at its focus into a plane wave. The infrared emitters used in the design are not point sources; therefore, the output is not a plane wave. However, the divergence of the beam reduces from ± 50 to $\pm 15°$. The infrared emitter used for generating the background spectrum is used without the parabolic reflector in order to produce a larger background spot. The divergence of the emitter used for generating background signatures is $\pm 50°$. Each of the infrared emitters generating the 3–5 μm spectrum are heated to a temperature of 775°C. The active area of the element is 1.5×3.5 mm and has an emissivity of 0.8. The total power emitted by these emitters, calculated using Planck's law, is 287 mW. Figure 3 shows the radiation spectrum of the emitter used for generating target signatures when heated to a temperature of 775°C. A midinfrared filter with a transmission of 85% in 3–5 μm band is used in front of these emitters. The emitters for generating the 8–12 μm spectrum are heated to a temperature of 900°C. The same types of emitters are used for generating spectra in the 3–5 and 8–12 μm bands. The total power produced by these emitters is 450 mW. Figure 4 shows the radiation spectrum of the emitter used for generating target signatures when heated to a temperature of 900°C. A far-infrared filter with transmission of 85% in the 8–12 μm band is used in front of these emitters. The emitter for generating background radiation is heated to a temperature of 80°C. The emitter has an active area of 1.8×1.8 mm and emissivity of 0.75. Therefore, it generates a total power of the order of 2 mW. Figure 5 shows the radiation spectrum of the emitter used for generating the background spectrum when heated to a temperature of 80°C. A broadband infrared filter with 80% transmission in the 3–12 μm band is used in front of the emitter generating background radiation. A transmission window with a transmission percentage of 80% is placed in front of all the emitters for mechanical protection.

As we can see from Eqs. (1–4), power emitted by the emitter between wavelengths λ_1 and λ_2 is related to the temperature and emissivity of the emitter. The percentage of power in the 3–5 μm band for an emitter with emissivity of 0.8 and heated to a temperature of 775°C is 36.1%. Therefore, the output power of a single emitter in the 3–5 μm band is 104 mW. Output power after passing through the midinfrared filter (transmission is 85% in 3–5 μm band) is 88 mW and after passing through the final transmission window is 70 mW (transmission is 80% in the 3–12 μm band). Two emitters are used to generate the desired power density in the 3–5 μm band at the device-under-test (DUT) plane. The percentage of power in the 8–12 μm band for an emitter with emissivity of 0.8 and heated to a temperature of 900°C is 8%. Therefore, the output power of the single emitter in the 8–12 μm band is 36 mW. Output power after passing through the far-infrared filter (transmission is 85% in 8–12 μm band) is 31 mW and after passing through the final transmission window is 25 mW (transmission is 80% in the 3–12 μm band). Therefore, six emitters are used to generate the desired power density in the 8–12 μm band at the target plane. The percentage of power in the 3–12 μm band for an emitter with emissivity of 0.75 and temperature of 80°C is 44%. Therefore, the power emitted by the emitter used to generate the background spectrum in the 3–12 μm band is approximately 0.9 mW. Output power after passing through the broadband infrared filter (transmission is 80% in the 3–12 μm band) is 0.72 mW and after passing through the final transmission window is 0.6 mW (transmission is 80% in the 3–12 μm band). It may be reiterated here that these values are for the chosen infrared emitters used to build the prototype hardware to validate the proposed concept. Similar calculations may be done for arrays employing different types of infrared emitters.

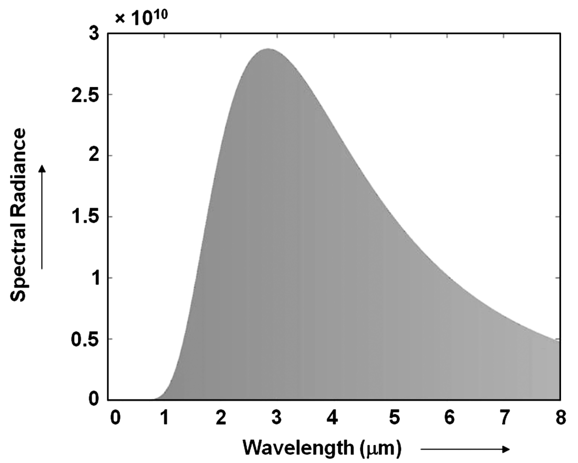

Fig. 3 Spectrum of the graybody emitter used for generating target signatures in the 3–5 μm band.

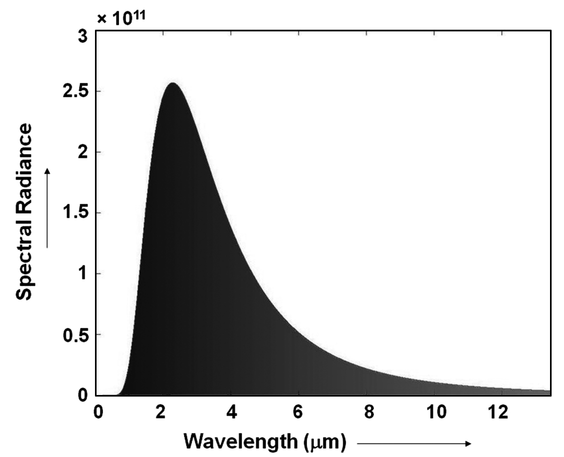

Fig. 4 Spectrum of the graybody emitter used for generating target signatures in the 8–12 μm band.

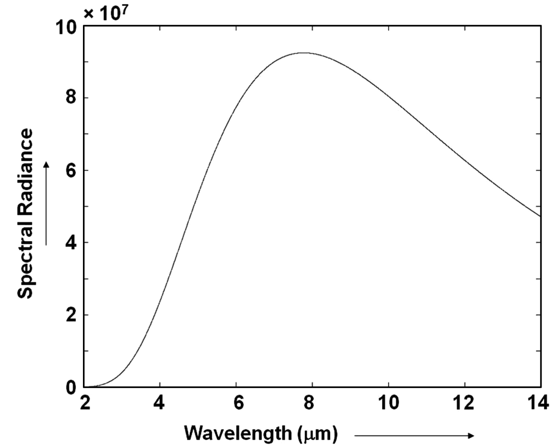

Fig. 5 Spectrum of the graybody emitter used for generating the background spectrum.

Interelement spacing in the array of emitters for given values of divergence angles is chosen to produce a nearly convergent infrared radiation spot at the front-end cross section of the DUT when kept at the desired distance from the exit of the infrared target simulator. In the present design, the interelement spacing of 1 cm and divergence of $\pm 15°$ ensures that convergence is greater than 90% at a distance of 1.0 m: i.e., the spots from different emitters overlap by more than 90%. Divergence angles of infrared emitters used for generating target and background signatures are selected to not only produce the desired power density values, but also to ensure that the spot size due to target signatures is much smaller than the spot size due to background radiation.

Figure 6 shows the convergence of spots for the target radiations in the 3–5 and 8–12 μm bands. Power available in this converged spot in the 3–5 and 8–12 μm bands is 126 and 135 mW, respectively, considering the power emitted by each element in the respective band, the number of elements used, the transmission coefficients of the bandpass filters and transmission window, and that only 90% of radiated power is available in the spot. Figure 4 shows the target radiation spots superimposed on the background radiation spot. Background power level is approximately 0.5 mW.

Figure 7 shows the 54-cm-diam spot produced due to target signatures in the 3–5 and 8–12 μm bands at the center of a 238-cm-diam spot produced due to background radiation in the 3–12 μm band at a distance of 1.0 m from the exit. These spot diameters are decided by the divergence of infrared emitters and distance from the

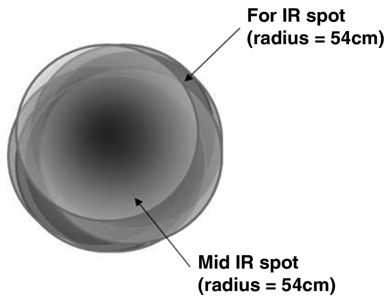

Fig. 6 Diagram showing convergence of individual radiation spots of the target spectrum.

exit. For divergence of $\pm 15°$ and 1.0 m distance, it would be 54 cm ($2 \times \tan 15° \times 100$ cm), and for divergence of $\pm 50°$, it would be 238 cm ($2 \times \tan 50° \times 100$ cm). For a spot diameter of 54 cm and power levels of 126 and 135 mW in the 3–5 and 8–12 μm bands, respectively, the power density in the 3–5 and 8–12 μm bands is approximately 56 $\mu W/cm^2$ each. For a spot diameter of 238 cm and a power level of 0.5 mW in background radiation, power density in background radiation is approximately 12 nW/cm^2 each.

The parameter control module shown in Fig. 2 comprises an embedded controller interfaced with the keypad and display and designed to generate control signals for the two-dimensional array. The prototype hardware employs a 128×128 liquid crystal display and a 3×3 matrix keypad. Any other suitable display and keypad could be used instead. The embedded controller can be programmed to produce the desired operational modes. In the proposed design, four operational modes are programmed. These include 1) target signatures in the 3–5 μm band without background, 2) target signatures in the 3–5 μm band with background, 3) target signatures in the 3–5 and 8–12 μm bands without background, and 4) target signatures in the 3–5 and 8–12 μm bands with background. Modes 1 and 2 are used for testing single-color infrared-guided missiles, and modes 3 and 4 are used for testing two-color infrared-guided missiles. Based on the operational mode selected through the keypad, the embedded controller generates a set of commands to operate a combination of controlled analog switches to allow the desired values of dc voltage to be applied to relevant infrared emitters. Desired dc voltages are generated by voltage regulator circuits that are part of the drive electronics module. The drive electronics module also comprises buffer circuits to provide the required drive current to the control inputs of analog switches.

Design Using Array of Infrared Light-Emitting Diodes

Another possible approach to design an infrared target simulator for testing the nonimaging types of infrared-guided missiles is to use an array of midinfrared LEDs (with different LEDs driven to generate infrared radiation in the specified wavelength spectrum) and a centrally located graybody emitter to generate the static background.

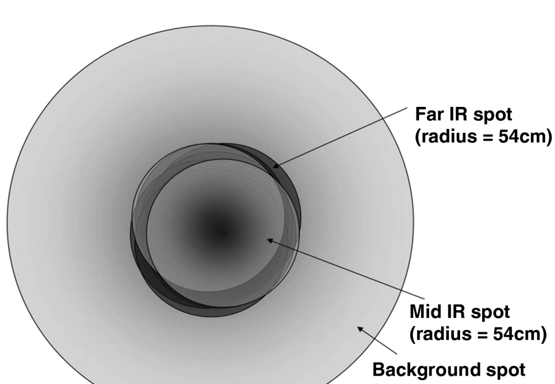

Fig. 7 Diagram showing radiation spots due to infrared signatures of target and background.

Each LED in the array generates a specific wavelength. Different LEDs in the array are chosen to have staggered peak emission wavelength over the wavelength region of interest. Typical FWHM (full width at half-maximum) linewidth of output radiation from these LEDs is in the range of 10 to 20% of the peak emission wavelength. Overlapping beams from these LEDs are combined to produce the desired wavelength spectrum. The LED-based design has two distinct advantages.

1) It does not require bandpass filters to get the desired spectral shape.

2) Output power from each LED, and therefore the total power, can be conveniently controlled by changing the input drive current, which allows the designer to build a device that can test the weapon over its full operational range.

Presently, these midinfrared LEDs are available only in the 1.6–7.0 μm band. Therefore, the proposed LED-based design is applicable to infrared target simulators for testing single-color infrared-guided missiles.

A number of manufacturers offer midinfrared LEDs. One such set of midinfrared LEDs comprising LED-30SC, LED-34SC, LED-36SC, LED-38SC, LED-42SC, and LED-47SC (Scitec), with corresponding peak emission wavelengths at 3.0, 3.4, 3.6, 3.8, 4.2, and 4.7 μm, could be used to generate the desired spectral output in 3–5 μm band for testing single-color infrared-guided missiles. These LEDs have a built-in lens that reduces the divergence of the emitted radiation. Some manufacturers offer midinfrared LEDs with built-in parabolic reflectors for the same purpose.

Figure 8 shows the block schematic arrangement depicting the midinfrared LED-based concept. A heterogeneous two-dimensional array of midinfrared LEDs and a single graybody emitter are the foundation of the system. Other major building blocks include the parameter control module and drive electronics module to operate the array of emitters and the protective optical window. The two-dimensional array of infrared emitters is used to generate the target signatures and background spectrum in the 3–5 μm band. Though the hardware built to validate the proposed design concept is configured around a 4×4 array of midinfrared LEDs and one graybody emitter, the concept is equally valid for a two-dimensional array of any size, as long as it meets the requirement of producing the required power density in the given spectral band with the desired spectral shape. Of the 16 midinfrared LEDs, there is one each of the types LED-30SC, LED-34SC, LED-36SC, and LED-38SC. There are four LEDs of the type LED-42SC and eight LEDs of the type LED-47SC. The number of elements producing 3–5 μm radiation depends upon the desired magnitudes of infrared radiation in the 3–5 μm band and the power level available from individual elements. The number of elements of each type in the array depends

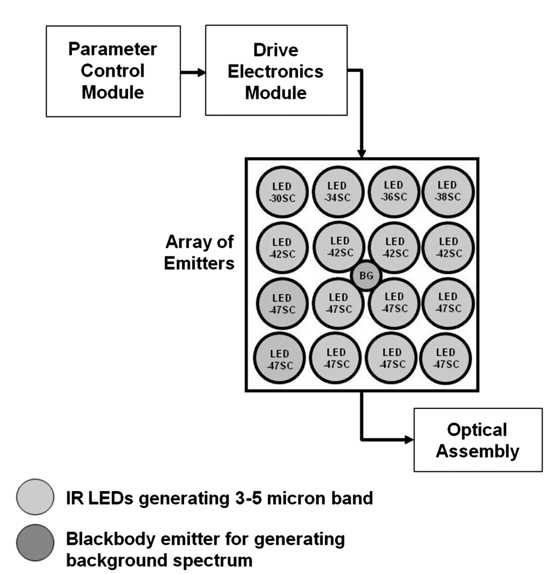

Fig. 8 Block schematic arrangement of design concept using array of midinfrared LEDs.

upon the continuous-wave power level available from individual LEDs of different peak emission wavelengths and the desired spectral shape.

Midinfrared LEDs are used without any bandpass filters, as the radiation from each individual LED has narrow linewidth around the peak wavelength. Figure 9 shows the radiated spectrum in the case of midinfrared LEDs chosen to build the prototype hardware. An infrared emitter used for generating background is used without a parabolic reflector, and a bandpass filter is placed in front of it, for reasons explained in the case of the first design. The peak of spectral output in the case of the graybody infrared emitter occurs at a wavelength dependent upon the temperature to which it is heated, which depends upon the dc voltage applied to the chosen type of solid-state infrared emitter. In the case of midinfrared LEDs, the drive current determines the output power. The LEDs chosen to generate the 3–5 μm band have FWHM of $\pm 20°$ without the lens and $\pm 10°$ with the lens. The graybody emitter used for generating the background has divergence of $\pm 50°$. A midinfrared bandpass filter placed in front of the background emitter has 80% transmission in the 3–5 μm band. The LEDs produce a radiation spot diameter of 0.35 m (area ≈ 0.1 m^2) for target signatures, and the graybody emitter produces a radiation spot diameter of 2.4 m (area $= 4.5$ m^2) for background at a DUT distance of 1.0 m.

The total power emitted by the LEDs is proportional to the drive current through them. The hardware developed has the option to choose from two different power levels for testing the missile at two different operational ranges. The total power in the radiation simulating target signatures is approximately 300 μW in one of the settings and 100 μW in the other setting. The second power setting is generated by changing the drive currents through the midinfrared LEDs. This current change is done by changing the switch position of the hardware. Power in background signatures is 0.6 mW in a spot diameter of 2.4 m. This results in background power density of 13.5 $\mathrm{nW/cm^2}$ and a settable target signature power density of approximately 312 and 104 $\mathrm{nW/cm^2}$.

The parameter control module is similar to the one described earlier in the case of the first design. Controlled analog switches in this case are the single-pole/double-throw type to allow selection of two different power densities of the target signatures through different current drives. The switch used to select the background is of the simple on/off type. Different combinations of keys on the keypad can be used to select the desired operational mode. The

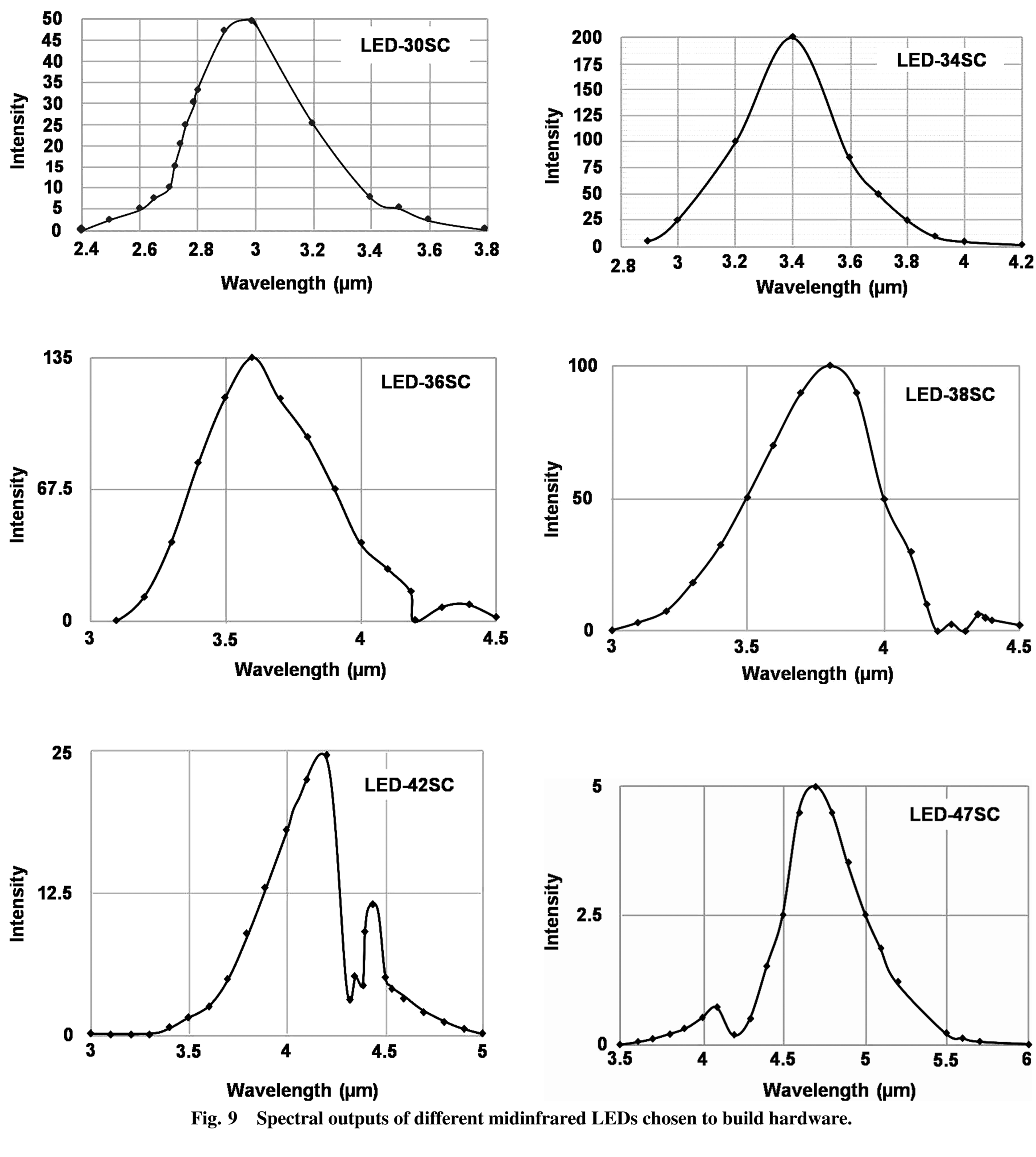

Fig. 9 Spectral outputs of different midinfrared LEDs chosen to build hardware.

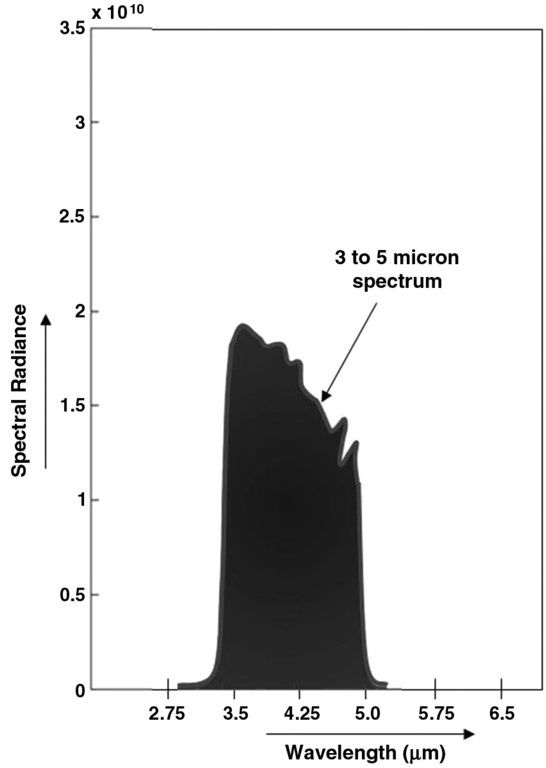

Fig. 10 Target infrared radiation spectrum in the 3–5 μm band without background radiation.

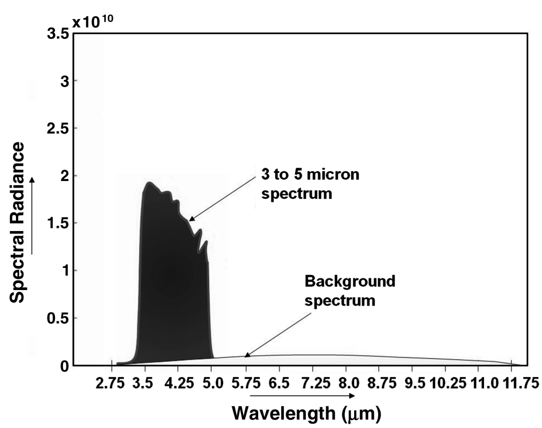

Fig. 11 Target infrared radiation spectrum in the 3–5 μm band with background radiation.

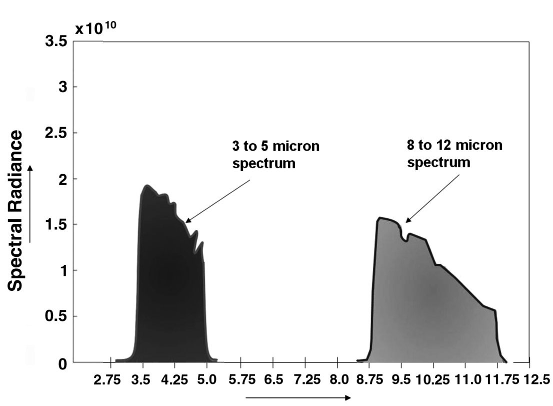

Fig. 12 Target infrared radiation spectrum in the 3–5 and 8–12 μm bands without background radiation.

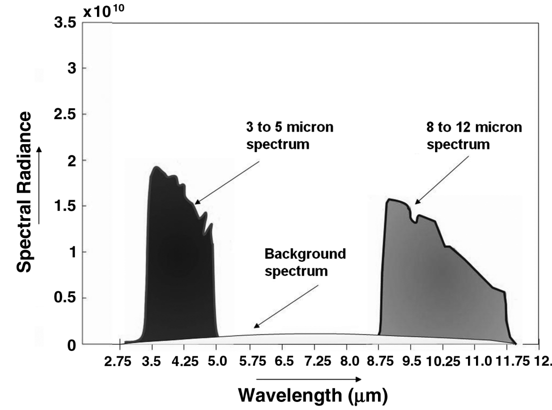

Fig. 13 Target infrared radiation spectrum in the 3–5 and 8–12 μm bands with background radiation.

keypad and the display module used to build the hardware to validate the proposed design concept are the same as those used in the case of the first design.

Hardware Evaluation

The prototype hardware built to validate the proposed concepts was evaluated for various performance parameters, which mainly include spectral distribution and power density.

Graybody-Emitter-Based Design

Figure 10 shows the infrared radiation spectrum for the operational mode generating target signatures in the 3–5 μm band without background infrared radiation. The measured power density is 56.5 $\mu\mathrm{W/cm^2}$. Figure 11 shows the infrared radiation spectrum generated for the operational mode generating target signatures in the 3–5 μm band with background infrared radiation. The measured

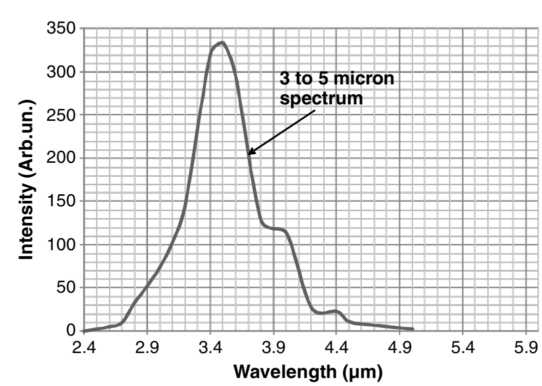

Fig. 14 Target infrared radiation spectrum in the 3–5 μm band without background radiation.

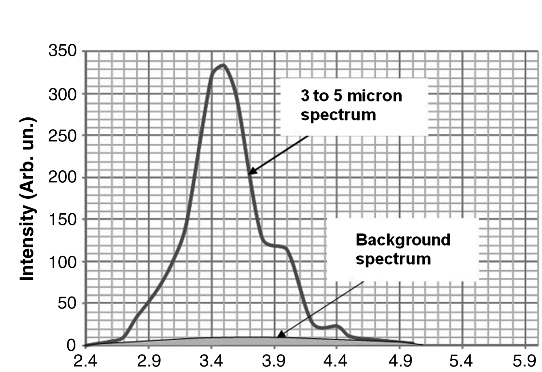

Fig. 15 Target infrared radiation spectrum in the 3–5 μm band with background radiation.

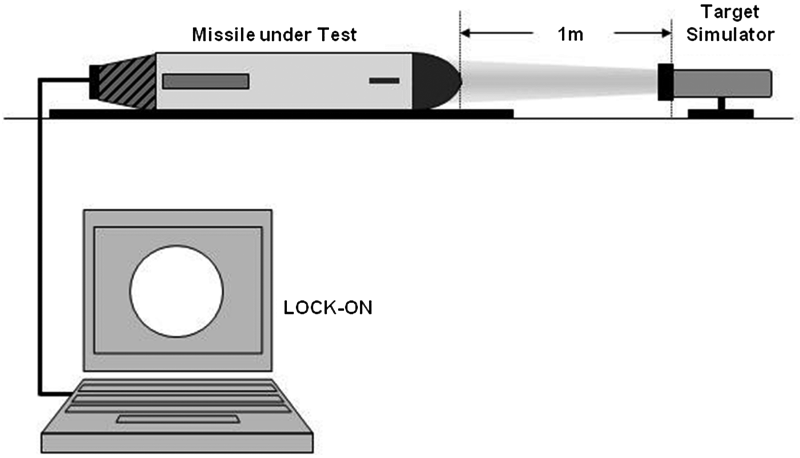

Fig. 16 Test setup for lock-on sensitivity check of infrared-guided missile seeker head.

power density is 56 $\mu W/cm^2$ in the case of the 3–5 μm band and 14 nW/cm^2 in the case of background radiation. Figure 12 shows the infrared radiation spectrum for the operational mode generating target signatures in the 3–5 and 8–12 μm bands without background infrared radiation. The measured power density is 55.5 $\mu W/cm^2$ in the case of the 3–5 μm band and 54.8 $\mu W/cm^2$ in the case of the 8–12 μm band. Figure 13 shows the infrared radiation spectrum for the operational mode generating target signatures in the 3–5 and 8–12 μm bands with background infrared radiation. The measured power density is 54.5 $\mu W/cm^2$ in the case of the 3–5 μm band, 54.8 $\mu W/cm^2$ in the case of the 8–12 μm band, and 14 nW/cm^2 in the case of background radiation. The measured values of power density in all cases closely match with the estimated values.

Midinfrared-LED-Based Design

Figures 14 and 15 show the spectral distribution of the target signatures in the 3–5 μm band without and with background radiation, respectively. The measured intensity versus wavelength curve closely matches with the estimated one. Measured power density in the 3–5 μm band is 310 nW/cm^2 for the first setting, which closely matches with theoretical values. The power density for the second setting was measured to be 95 nW/cm^2, which again matches with the theoretical estimate. The prototype hardware in the two cases was used to perform lock-on sensitivity check on the seeker head of a single-color infrared-guided missile of foreign origin. Figure 16 shows the test setup.

Conclusions

Two design approaches to building an infrared target simulator for performing a preflight serviceability check on both single-color and two-color infrared-guided missiles without the need for disassembling them from the launch platform are presented in this paper. The resulting hardware is intended to be portable, which is an essential requirement for carrying out serviceability checks in strap-on condition. In addition, the proposed designs generate the desired infrared signatures of the target in the presence of background noise, thus simulating the real battlefield conditions and overcoming limitations of similar portable devices that are available commercially or discussed in literature.

References

[1] Rao, G. A., and Mahulikar, S. P., "New Criterion for Aircraft Susceptibility to Infrared Homing Missiles," *Aerospace Science and Technology*, Vol. 9, No. 8, Nov. 2005, pp. 701–712.
doi:10.1016/j.ast.2005.07.005

[2] Pollock, D. H., "Countermeasures Systems," *The Infrared Electro-Optical Systems Handbook*, 1st ed., Vol. 7, SPIE, Bellingham, WA, 1993, pp. 162–165.

[3] Sturlesi, D., and Pinsky, E., "Target Scene Generator (TSG) for Infrared Seeker Evaluation," *Technologies for Synthetic Environments: Hardware-in-the-Loop Testing II*, Proceedings of SPIE, Vol. 3084, SPIE, Bellingham, WA, July 1997, pp. 111–119.
doi:10.1117/12.280941

[4] Rao, G. A., and Mahulikar, S. P., "Effect of Atmospheric Transmission and Radiance on Aircraft Infrared Signatures," *Journal of Aircraft*, Vol. 42, No. 4, July–Aug. 2005, pp. 1064–1054.
doi:10.2514/1.7515

[5] Bell, W. A., and Glasgow, B. B., "Impact of Advances in Imaging Infrared Detectors on Anti-Aircraft Missile Performance," *Infrared Imaging Systems: Design, Analysis, Modeling, and Testing X*, Proceedings of SPIE, Vol. 3701, SPIE, Bellingham, WA, April 1999, pp. 244–253.
doi:10.1117/12.352977

[6] Longair, M. S., "Black-body Radiation up to 1895," *Theoretical Concepts in Physics: An Alternative View of Theoretical Reasoning in Physics*, 2nd ed., Cambridge Univ. Press, Cambridge, England, U.K., 2003, pp. 283–301.

[7] Longair, M. S., "1895–1900: Planck and the Spectrum of Black-Body Radiation," *Theoretical Concepts in Physics: An Alternative View of Theoretical Reasoning in Physics*, 2nd ed., Cambridge Univ. Press, Cambridge, England, U.K., 2003, pp. 303–325.

[8] Maini, A. K., and Agrawal, V., "Portable Electro-Optic Device for Performing Serviceability Check on IR Guided Missiles," *Opto-Electronics Review*, Vol. 17, No. 3, Nov. 2009,
doi:10.2478/s11772-008-0079-z

A. Ketsdever
Associate Editor